Effects of compression cycles on the atomic mobility in metallic glasses

Francesco Delogu*
Dipartimento di Ingegneria Chimica e Materiali, Università di Cagliari, piazza d'Armi, I-09123 Cagliari, Italy
(Received 25 September 2008; published 27 February 2009)

Molecular-dynamics methods have been employed to investigate atomic displacement mechanisms in $Ni_{50}Zr_{50}$ metallic glasses both in the absence and in the presence of an elastic shear stress. Calculations were performed on systems subjected to a different number of hydrostatic compression cycles. In all the cases, local collective rearrangements of Ni and Zr atoms connected in clusters are observed. Numerical findings indicate that rearrangements occurring in unstrained and strained systems involve roughly the same regions. In addition, compression cycles produce the same effects on atomic mobility in unstrained and strained systems. This suggests the existence of regions characterized by a particular structural instability that determines a significant correlation of atomic displacements in unstrained and strained systems.

DOI: 10.1103/PhysRevB.79.064205 PACS number(s): 61.43.Fs, 66.10.−x, 64.70.P−, 66.30.−h

I. INTRODUCTION

Metallic glasses combine the amorphous structure with remarkable mechanical properties.[1–4] Their elastic moduli are in fact on the same order of magnitude of the ones of the crystalline counterparts, but the room-temperature strength is larger.[4–6] Unfortunately, they also exhibit a tendency to strain localization that severely limits the room-temperature ductility.[4–7] As a consequence, strained metallic glasses can nucleate shear bands and possibly undergo a brittle failure.[4–7] This behavior must be related to the absence of long-range structural order, which suppresses the dislocation-mediated deformation mechanisms characteristic of crystalline phases.[2–4] Deformation promotes instead high-energy atomic rearrangements localized in shear transformation zones (STZs).[4–19] These can be regarded as groups of 10 to 100 atoms that undergo a transition between two relatively low-energy configurations separated by a relatively high-energy barrier.[4–19]

At present, the research on STZs is central to the field of metallic glasses and matter of a lively debate.[4,5] A detailed understanding of STZ activity is in fact a crucial issue to better understand the mechanism underlying the formation of shear bands and contrast the undesired brittle behavior.[4–7] Nevertheless, no definite answer has been given yet to several fundamental questions. Open questions are, for example, the size, the shape, and the activation mechanisms of STZs as well as the relationship between potential STZs and local atomic arrangements.[4,5]

As for the latter aspect, the inhomogeneous character exhibited by the amorphous structure on the atomic scale[1–3] is thought to play a key role. Atomic arrangements are expected to possess an intrinsic degree of instability against local rearrangements.[1–3,5–14] The first STZs operating under deformation can be therefore thought to involve preferentially those particular sites, or groups of atoms, characterized by the highest structural instability and then more prone to structural changes. Under such circumstances, local irreversible plastic events in which atoms cooperatively modify their positions could take place even at small shear strains and, in the limit, under purely thermal activation.

A possible way to ascertain the existence of particularly unstable regions in the metallic glass structure relies upon the identification of atoms undergoing local displacements both in the absence and in the presence of an applied shear stress. Should such atoms be to a large extent the same, an intriguing connection between thermal mobility and displacements induced by shear would emerge. It would point out that thermal mobility in the absence of shear stress and atomic rearrangements under deformation conditions are determined, or at least significantly affected, by the structural stability of local atomic arrangements. This not only would open the door to a correlation between thermal mobility and STZs but also could allow to identify potential STZs on the basis of local structural features.

The present work employs Molecular-dynamics methods precisely to investigate the above-mentioned scenario for a model $Ni_{50}Zr_{50}$ metallic glass. To such aim, amorphous structures were suitably generated and relaxed. Successively, the mobility of atomic species under simple thermal activation as well as under shear deformation was studied. To strengthen the hypothesis that metallic glasses contain atomic arrangements with different structural stability, initial relaxed configurations were also subjected to hydrostatic compression cycles. These could in fact be able to induce the rearrangement of at least part of most unstable regions. Should this be the case, the number of atoms undergoing a rearrangement under thermal activation or under shear deformation should in general decrease with the number of compression cycles carried out. Such decrease could provide further information on both thermal and shear-induced rearrangements.

Two additional introductory comments are in need to suitably frame this work. First, calculations were carried out at a temperature relatively close to the one of glass transition. In fact, only such temperature regime allows significant mass transport in the absence of shear stress. Second, the structural response of the model metallic glass is studied only at small strains. Unstable regions as well as the relationship between thermal and shear-induced atomic rearrangements should be indeed more clearly identified precisely under such conditions.

II. NUMERICAL SIMULATIONS

A many-body semiempirical tight-binding potential was used to reproduce interatomic forces.[20] The cohesive energy E was expressed as

$$E = \sum_{i=1}^{N} \left\{ \left[\sum_{j=1}^{N} A_{\alpha\beta} e^{-p_{\alpha\beta}(r_{ij}/r_{0,\alpha\beta}-1)} \right] - \left[\sum_{j=1}^{N} \xi_{\alpha\beta}^2 e^{-2q_{\alpha\beta}(r_{ij}/r_{0,\alpha\beta}-1)} \right]^{1/2} \right\}, \quad (1)$$

where r_{ij} represents the distance between atoms i and j, $r_{0,\alpha\beta}$ is the distance between nearest neighbors of species α and β at 0 K, and N is the total number of atoms. The potential parameters $A_{\alpha\beta}$, $\xi_{\alpha\beta}$, $p_{\alpha\beta}$, and $q_{\alpha\beta}$ for pure and cross interactions, computed within a cut-off radius of about 0.8 nm, were taken from literature.[20–22] Such parameters were optimized to satisfactorily best fit the thermodynamic and mechanical properties of the equilibrium crystalline phases of Ni and Zr as well as of their intermetallics.[20–22] However, amorphous structures can also be reliably studied.[20–22] Accordingly, although more accurate force schemes are available to investigate Ni-Zr systems,[23] the tight-binding potential is well suited for the qualitative purposes of the present investigation.

Calculations were carried out in the NPT ensemble with number of atoms N, pressure P, and temperature T constant.[24,25] Equations of motion were solved with a fifth-order predictor-corrector algorithm[26] and a time step of 2 fs. A relatively large $Ni_{50}Zr_{50}$ metallic glass consisting of 131 064 at. arranged in a $13.3 \times 6.5 \times 27.2$ nm^3 simulation cell was employed to have a significant statistics on the behavior of atomic species. This allowed, in particular, a satisfactory characterization of the atomic mobility both in the absence and in the presence of an applied shear stress without carrying out repeated averages over different time intervals. The metallic glass was prepared by quenching the corresponding liquid system from 2000 to 700 K at a rate $\dot{Q}$ of 2 K ps^{-1} and null pressure. Periodic boundary conditions (PBCs) (Ref. 26) were applied along the x, y, and z Cartesian directions. The glass transition took place at about 1020 K, in accordance with previous work.[27] Once the temperature reached 700 K, the system was relaxed for 50 ps to produce the initial unstrained configuration. Starting from the latter, ten different unstrained configurations were generated by carrying out ten compression cycles. Any compression cycle consists of three stages. First, the pressure P is raised at a rate of 0.1 GPa ps^{-1} up to a P_{max} value of about 12 GPa. Second, P is kept constant at P_{max} for a time period Δt_P of 50 ps. Finally, a zero pressure condition is restored by removing the load. The pressure generally takes about 70 ps to attain the zero value. In any case, the metallic glass was relaxed successively for additional 30 ps to give the third stage of each compression cycle a total duration of 100 ps. The systems did not suffer, in the relaxation stage, any severe volume oscillation. Rather, the pressure reaches the zero value gradually, probably due to the relatively large size of the system. It is only after the relaxation stage that the atomic mobility is studied both in the absence and in the presence of applied shear stress over time intervals as long as 1 ns.

The characteristics of compression cycles leave the door open to a possible comparison with experimental studies where a load is gradually applied to a sample, the maximum pressure kept constant for a given time interval and finally the load suddenly removed. It should be also noted that P_{max} and Δt_P values different from the ones mentioned above were used, though not systematically, to obtain an indication of their effect on the system dynamics.

It is here worth noting that the mobility of atomic species was studied after the Nosè thermostat was removed. Such thermostat is indeed based on a stochastic control of the average temperature,[25] and its use could affect the distribution of kinetic energy among the atoms. The evaluation of the kinetic temperature T after the thermostat removal did not point out, however, any temperature drift. The study of mobility was associated to a characterization of atomic volumes under the hypothesis that these are important quantities in determining the possibility of displacement for individual atoms. The atomic volumes were estimated via a Voronoi space tessellation.[28]

All the computations were carried out at least twice to explore different initial conditions. However, calculations at cooling and compression rates of 1 K ps^{-1} and 0.05 GPa ps^{-1} produced similar results, which will not be explicitly discussed in the work.

III. CALCULATIONS IN THE ABSENCE OF SHEAR STRESS

The mobility of Ni and Zr atoms in unstrained configurations was measured by estimating the diffusion coefficient D through a quantification of the root-mean-square (rms) displacements[26] of individual atoms. Calculations were performed at four different pressure values, namely, 0, 4, 8, and 12 GPa. These values were reached by increasing the pressure at a nominal rate of 0.1 GPa s^{-1}. Once we attained the desired pressure, the system was relaxed for 50 ps and rms displacements, successively evaluated over time intervals of 20 ps long. The calculation of D at different pressures permitted estimation of the activation volume for diffusion $\Omega_{act} \approx -k_B T(\partial \ln D/\partial P)_T$, where k_B represents the Boltzmann constant. The Ω_{act} value was determined by the slope of the plot obtained by reporting the logarithm of D, $\ln D$, as a function of P.[29] The procedure described above was repeated for all the unstrained configurations subjected to m compression cycles. The Ω_{act} estimates for the various unstrained configurations are shown in Fig. 1 as a function of the number m of compression cycles. It can be seen that Ω_{act} undergoes a progressive increase with m, which points out a decrease in atomic mobility. Additional Ω_{act} data for the unstrained configurations with $m=0$, 3, and 8 were obtained using P_{max} and Δt_P values, respectively, equal to 18 GPa and 100 ps. The resulting Ω_{act} values, also shown in Fig. 1, are larger than the others. This suggests that Ω_{act} increases with both P_{max} and Δt_P, with being Δt_P more influent than P_{max}. The Ni and Zr species exhibit different Ω_{act} values, which

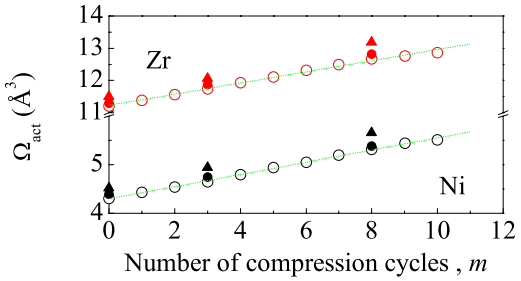

FIG. 1. (Color online) The activation volume Ω_{act} for Ni and Zr as a function of the number m of compression cycles. Best-fitted lines are also shown. Additional points at m equal to 0 and 3 refer to P_{max} (●) and Δt_P (▲) values equal to 18 GPa and 75 ps, respectively.

amount to about 4.5 and 11.2 Å^3, respectively. These values must be compared with the average Ni and Zr atomic volumes $\bar{\Omega}_{Ni}$ and $\bar{\Omega}_{Zr}$ obtained from the Voronoi tessellation,[28] which are instead approximately equal to about 11.5 and 23.5 Å^3. In accordance with previous work,[29–31] a cooperative diffusion scenario can be inferred from the aforementioned Ω_{act} and $\bar{\Omega}$ values. Larger Ω_{act} values are indeed expected for diffusion mechanisms mediated by vacancylike defects.[29–31]

In light of this, atomic mobility was characterized by resorting to the self-part of the van Hove function $G_s(l,\Delta t)$ and the non-Gaussian parameter $\alpha_2(\Delta t)$. These quantities measure, respectively, the probability for atoms to cover a distance l in a time interval Δt and the deviation of $G_s(l,\Delta t)$ from the Gaussian shape.[32,33] The behavior exhibited by Ni and Zr atoms is similar. For both species $G_s(l,\Delta t)$ develops a second peak at the distance $r_{nn,\alpha\alpha}$ of nearest neighbors indicated by the partial $\alpha\alpha$ pair-correlation function (PCF).[26] At the same time, also $\alpha_2(\Delta t)$ attains a maximum value. This points out that Ni and Zr atoms undergo a heterogeneous correlated motion in groups on a time scale measured by τ.[32,33] For both Ni and Zr, the time period τ is roughly equal to 24 ps. Moreover, τ is independent of the number m of compression cycles and of their characteristic parameters P_{max} and Δt_P.

The atoms participating in correlated motion were identified by using the conditions $0.35r_{nn} < |\boldsymbol{r}_i(\tau) - \boldsymbol{r}_i(0)| < 0.86r_{min}$ and $\min[|\boldsymbol{r}_i(\tau) - \boldsymbol{r}_j(0)|, |\boldsymbol{r}_j(\tau) - \boldsymbol{r}_i(0)|] < 0.43r_{nn}$.[32,34] Here $\boldsymbol{r}_i(t)$ is the ith atom position at time t, whereas r_{nn} and r_{min} are, respectively, the average nearest-neighbor distance and the first-minimum distance indicated by the global PCF. The former condition selects the atoms mobile within the time period τ. The latter identifies instead the pairs of atoms with remaining nearest neighbors in correlated displacements on the same time scale.[32,34] As for the former condition, it should be noted that the value $0.35r_{nn}$ roughly identifies the amplitude of thermal vibrations. It follows that the displacement of a given atom is considered as part of a collective motion only if it is longer than the thermal vibration amplitude. The value $0.86r_{min}$ represents instead a limit to the length of collective displacements. The condition exploiting such limit originates from the need to distinguish between cooperative motion and individual atomic displacements due to a vacancylike mechanism. This latter is however practically absent in metallic glasses. In accordance, in all the cases investigated the percentage of displacements longer than $0.86r_{min}$ was below the 1%. Finally, the distance $0.43r_{nn}$ used in the second condition assures that collectively displacing atoms remain very close after the displacement has occurred. It should be noted here that the numerical coefficients satisfactorily discriminate between collective rearrangements and other forms of motion,[34] but slightly different values also can be profitably used. In all the cases, the qualitative inferences on the atomic dynamics that can be obtained from such analyses do not change.

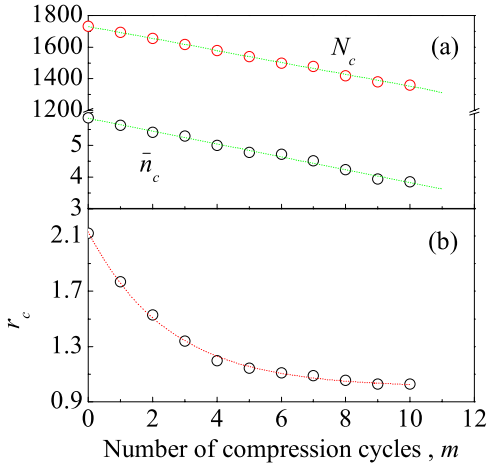

FIG. 2. (Color online) (a) The number N_c of mobile atom clusters and their average size $\bar{n}_c$ in unstrained configurations and (b) the ratio r_c between the number of Ni and Zr atoms participating in correlated motion in unstrained configurations as a function of the number m of compression cycles. Best-fitted curves are also shown.

It must be also noted that cooperatively displacing atoms can be identified only *a posteriori* after the system has evolved according to its dynamics through the analysis of stored atomic positions. Such analyses are necessarily cumbersome, and the method is relatively far from the ideal accuracy. For example, a source of inaccuracy is the length of the time period τ. It only represents an average value, and unavoidably there will be atomic species undergoing cooperative displacements over either longer or shorter time intervals. Their number is however acceptably small, amounting approximately to 3%. Other sources of inaccuracy produce as well only small uncertainties, enabling the methods applied to satisfactorily work out the qualitative features of atomic dynamics.

The analyses performed indicate that mobile species form connected groups, or clusters in which any given atom is nearest neighbor of at least another one. The number N_c of such clusters and their average size $\bar{n}_c$ are affected by the number m of compression cycles undergone by the atomic system. In particular, the data reported in Fig. 2(a) as a function of m show that both N_c and $\bar{n}_c$ exhibit a linear decrease. This suggests that the decrease in the atomic mobility is related to the average decrease in the number of atomic species participating in the collective motion.

Additional information is given by the ratio r_c of Ni-to-Zr atoms participating in cooperative motion, which describes

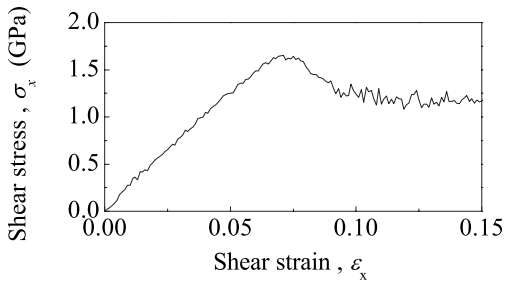

FIG. 3. The stress σ_x along the x Cartesian direction as a function of the strain ε_x.

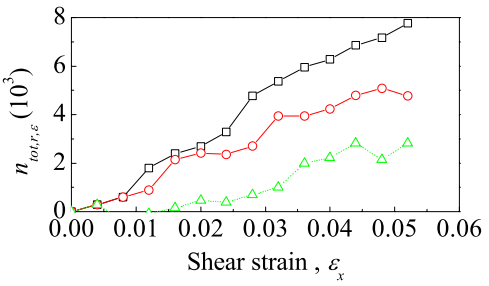

FIG. 4. (Color online) The total number $n_{\mathrm{tot},r,\varepsilon}$ of atoms rearranging their positions at least once as a function of the strain ε_x. Data refer to strained configurations that have undergone zero (□), five (○), and ten (△) compression cycles.

the chemical composition of the atomic clusters undergoing collective displacements. As shown in Fig. 2(b), r_c decreases from about 2.12 to about 1. The decrease in atomic mobility is thus associated with a decrease in the number of Ni atoms involved in cooperative displacements. It is here worth remembering that Ni and Zr atoms in metallic glasses exhibit a different mobility,[29–31] partly due to the different atomic size. Accordingly, Ni is often referred to as the fast diffuser.[29–31] Therefore, the r_c decrease suggests that the gradual reduction in atomic mobility produced by compression cycles must be ascribed to mobile Ni atoms.

IV. CALCULATIONS IN THE PRESENCE OF SHEAR STRESS

Mechanical deformation was obtained by applying a shear stress to any given unstrained configuration that has undergone m compression cycles. Strained configurations were thus correspondingly generated. Following previous work,[35] rigid reservoir regions 1.5 nm thick were defined at the top and the bottom of the simulation cell along the z Cartesian direction. PBCs were instead applied along the remaining ones. Shearing along the x Cartesian direction was produced by imposing to reservoirs incremental displacements at a nominal strain rate of about 0.14 ns^{-1}. Reservoirs were kept at constant distance. Atomic mobility was quantified by comparing via affine transformations the atomic positions in successive configurations. This permits application of the same conditions used to identify mobile atoms in unstrained confgurations.[32,34] In this case, however, such conditions use atomic positions $\boldsymbol{r}_i(t)$ implicitly accounting for the relative displacement due to shear deformation. A strain ε_x interval between 0 and 0.052 was considered to deal with elastic deformation. The choice of such interval is motivated by the shape of the stress-strain curve of the metallic glass shown in Fig. 3. It can be seen that the roughly linear increase in the stress σ_x, which describes the elastic deformation regime, extends up to a strain ε_x value of about 0.06. The curve exhibits then a maximum due to a yield and a flow state regime of plastic deformation, the characteristics of which compare well with literature data.[36]

Since the beginning of shearing, the progressive accumulation of strain ε_x along the x Cartesian direction is accompanied by atomic rearrangements characterized by irreversible changes in the position of atomic species. Structural modifications were initially characterized by evaluating the total number $n_{\mathrm{tot},r,\varepsilon}$ of mobile atoms that rearrange their positions at least once. The case of a few strained configurations is shown in Fig. 4, where $n_{\mathrm{tot},r,\varepsilon}$ is reported as a function of the strain ε_x. A monotonic $n_{\mathrm{tot},r,\varepsilon}$ increase is observed, the rate of which depends on the number m of compression cycles undergone by strained configurations. More specifically, the rate of $n_{\mathrm{tot},r,\varepsilon}$ increase decreases with m.

Further insight into the dynamics of individual atomic rearrangements was gained by evaluating the instantaneous number $n_{r,\varepsilon}$ of atoms involved in such local processes as a function of a scaled time t_r. Used only for simplicity, this represents the time elapsed since the beginning of a given local rearrangement. Its zero corresponds then to the instant at which the rearrangement starts. Typical results are shown in Fig. 5. Only a relatively small number of atoms, connected in clusters and undergoing collective displacements, are involved in local bursts of atomic mobility. The average size $\bar{n}_{r,\varepsilon}$ of the clusters observed in a strained configuration is not sensitive to strain ε_x, keeping an approximately constant value as the latter increases. It undergoes instead a linear decrease with the number m of compression cycles undergone by the configuration, as shown in Fig. 6(a) where $\bar{n}_{r,\varepsilon}$ is reported as a function of m. The number $N_{r,\varepsilon}$ of mobile atom clusters as well as the ratio $r_{r,\varepsilon}$ of Ni-to-Zr mobile atoms at any given strain ε_x, reported in Figs. 6(a) and 6(b), respectively, as a function of the number m of compression cycles, exhibit also a decrease. The change in $r_{r,\varepsilon}$ with the strain ε_x

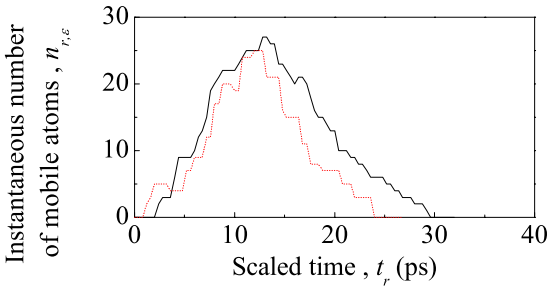

FIG. 5. (Color online) The instantaneous number $n_{r,\varepsilon}$ of mobile atoms involved in given individual rearrangements as a function of the rescaled time t_r. Curves refer to atomic rearrangements occurring in configurations experiencing a strain ε_x value equal to 0.03 that have undergone two (black, solid) and eight (red, dotted) compression cycles.

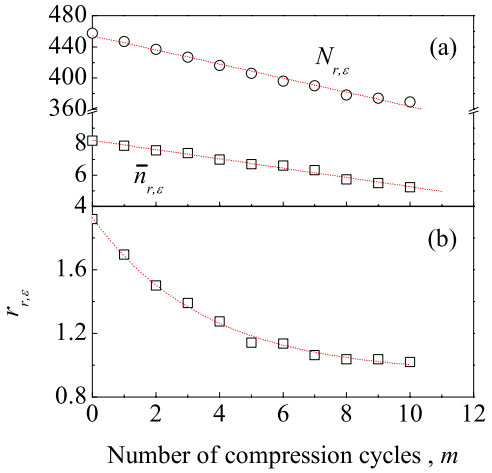

FIG. 6. (Color online) (a) The number $N_{r,\varepsilon}$ of mobile atom clusters and their average size $\bar{n}_{r,\varepsilon}$ and (b) the ratio $r_{r,\varepsilon}$ between the number of Ni and Zr atoms participating in correlated motion as a function of the number m of compression cycles. Data refer to configurations experiencing a strain ε_x value equal to 0.02. Best-fitted lines are also shown.

for a configuration that has undergone two compression cycles is instead shown in Fig. 7. Analogous results were obtained for strained configurations that have undergone a different number of compression cycles.

V. ATOMIC MOBILITY AND COMPRESSION CYCLES

According to the evidences as yet discussed, atomic displacements in unstrained and strained configurations share various common features. First, they exhibit a cooperative character, with mobile atoms connected in clusters. Second, the number and average size as well as the chemical composition of such clusters are sensitive to compression cycles. The similar responses of unstrained and strained configurations support the hypothesis that metallic glasses are complex assemblies of local atomic arrangements with a defined hierarchy of stability. Correspondingly, most unstable arrangements rearrange even under the effects of small thermal or mechanical perturbations.

A comparison between collective displacements was carried out to point out possible correlations between mobile

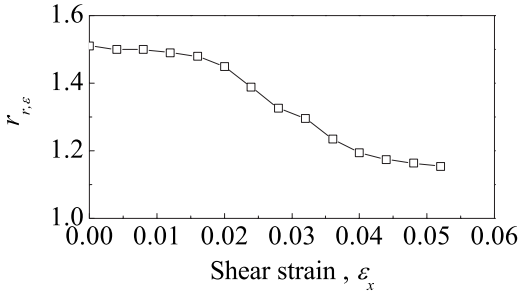

FIG. 7. The ratio $r_{r,\varepsilon}$ between the number of Ni and Zr atoms participating in correlated motion as a function of the strain ε_x. Data refer to strained configurations that have undergone two compression cycles.

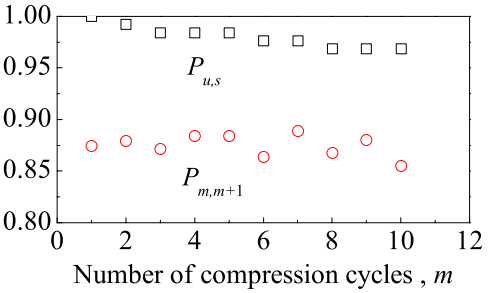

FIG. 8. (Color online) The probabilities $P_{u,s}$ (□) and $P_{m,m+1}$ (○) as a function of the number m of compression cycles. Data were calculated by considering configurations strained at a ε_x value of 0.03.

atoms in unstrained and strained configurations and identifying possible unstable regions. To such aim, the probabilities $P_{u,s}$ and $P_{m,m+1}$ were defined. The former represents the probability for a given atom that has participated in a rearrangement in a given unstrained configuration to undergo a rearrangement also in the corresponding strained configuration. The latter represents instead the probability for a given atom rearranging in a given unstrained configuration as well as in the corresponding strained one to lose its mobility simultaneously in the unstrained and strained configurations as a consequence of a compression cycle.

It is here worth noting that the evaluation of the above mentioned probabilities is complicated by two aspects. First, both $P_{u,s}$ and $P_{m,m+1}$ are expected to depend on the strain ε_x. Second, the number of mobile atoms in unstrained configurations is generally smaller than in strained ones. Such complications have been dealt with by using the number of mobile atoms in unstrained configurations as a reference value. The calculation of $P_{u,s}$ reduces then to the identification in strained configurations of the same atoms that have undergone a rearrangement in unstrained configurations. Such atoms are counted only if they have rearranged also in strained configurations. $P_{u,s}$ is finally obtained by normalizing the total number of atoms rearranging in strained configurations to the total number of atoms rearranging in unstrained configurations. Correspondingly, $P_{u,s}$ would be equal to 1 when the atoms rearranging in unstrained and strained configurations are the same. $P_{m,m+1}$ can be instead calculated by identifying in strained configurations the same atoms that have lost their mobility in unstrained ones after a compression cycle. If such atoms have lost their mobility also in strained configurations, they are counted. $P_{m,m+1}$ is finally obtained by normalizing the total number of immobilized atoms in strained configurations to the total number of atoms immobilized in unstrained configurations. Therefore, $P_{m,m+1}$ would be equal to 1 when the atoms that have lost their mobility in unstrained and strained configurations as a consequence of a compression cycle are the same.

The $P_{u,s}$ and $P_{m,m+1}$ values obtained are shown in Fig. 8 as a function of the number m of compression cycles. It can be seen that, although $P_{u,s}$ undergoes a slight decrease with m, its values keep close to 1. Thus, most of atoms involved in collective displacements in unstrained configurations also participate in cooperative motion in strained ones. $P_{m,m+1}$

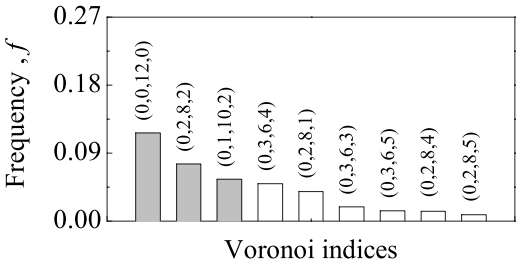

FIG. 9. The frequency f of the most representative Voronoi polyhedra for the unstrained configuration that has not undergone compression cycles. Bars pertaining to *ih* and *ih*-like polyhedra are in light gray.

values are slightly smaller than $P_{u,s}$ ones, which means that the atoms that lose their mobility in cooperative rearrangements in unstrained and strained configurations are approximately the same. The data shown in Fig. 8 were obtained by considering a configuration strained at a ε_x value of 0.03, but analogous results are obtained with other strained configurations.

The evidences concerning $P_{u,s}$ and $P_{m,m+1}$ suggest that cooperative rearrangements in the absence of shear stress, i.e., under simple thermal activation, and in the presence of shear stress, i.e., under mechanical deformation, involve approximately the same regions of metallic glass. The number of such regions is decreased by compression cycles, which are then able to modify the structure of local atomic arrangements and thus affect atomic mobility.

VI. LOCAL STRUCTURES AND ATOMIC MOBILITY IN UNSTRAINED CONFIGURATIONS

The decrease in the ratios r_c and $r_{r,\varepsilon}$ between Ni and Zr mobile atoms with the number m of compression cycles represents a signature of the effects of individual compression cycles. The decrease in the number of mobile Ni atoms plays thus a key role in the overall atomic mobility decrease due to structural modifications of local atomic arrangements. For this reason, the coordination of Ni atoms in unstrained configurations was characterized in detail by taking advantage of the space tessellation with Voronoi polyhedra.[28] The different Voronoi polyhedra were described in terms of the specific Voronoi indices (s,t,v,w), which indicate respectively the number of faces with three, four, five, and six vertices.[28] The frequency f of the different Voronoi polyhedra observed in the unstrained configuration that has not undergone compression cycles is shown in Fig. 9. It can be seen that a significant fraction of polyhedra has an icosahedral (*ih*) geometry. However, the Ni average coordination number is quite far from 12. It approaches indeed to 9 in accordance with previous work.[37] The coordination number of Zr atoms, roughly equal to 14, also agrees with molecular-dynamics data given in the literature.[38] Compression cycles determine only little changes in the distribution of Voronoi polyhedra, which mostly concern the (0,0,12,0), (0,2,8,2), and (0,1,10,2) *ih* and *ih*-like coordination shells. The frequency f of these Voronoi structures varies with the number m of compression cycles as shown in Fig. 10. The fractions of *ih* polyhedra with indices

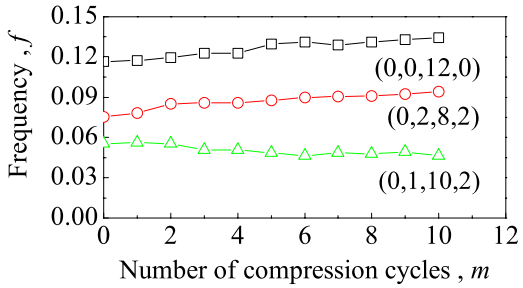

FIG. 10. (Color online) The frequency f of *ih* and *ih*-like Voronoi polyhedra in unstrained configurations as a function of the number m of compression cycles. Polyhedra are specified by their Voronoi indices.

(0,0,12,0) and (0,2,8,2) gradually increase, whereas the fraction of *ih*-like (0,1,10,2) ones decreases. On the whole, the fraction of *ih* polyhedra increases however from about 0.24 to 0.27.

It is now worth noting that the number $n_{\mathrm{Ni},c}$ of mobile Ni atoms in unstrained configurations and the one $n_{\mathrm{Ni},r,\varepsilon}$ of mobile Ni atoms in strained configurations for any given strain ε_x correlate quite well with the number $n_{\mathrm{Ni},ih}$ of Ni atoms with *ih* and *ih*-like coordinations. As shown in Fig. 11, $n_{\mathrm{Ni},c}$ and $n_{\mathrm{Ni},r,\varepsilon}$ decrease indeed linearly as $n_{\mathrm{Ni},ih}$ increases. This behavior can be tentatively related to the relatively small volume of Ni atoms with *ih* and *ih*-like coordinations, which amounts on the average only to about 0.8 $\bar{\Omega}_{\mathrm{Ni}} \approx 9.6$ Å^3. The consequence of such small value on the mobility of Ni atoms with *ih* and *ih*-like coordinations can be inferred by estimating the activation volume $\Omega_{\mathrm{act,Ni},ih}$ for the displacement of these species in unstrained configurations. Substantially independent of compression cycles undergone by unstrained configurations, $\Omega_{\mathrm{act,Ni},ih}$ takes an average value of about 6.2 Å^3 that is significantly larger than the average activation volume Ω_{act} of 4.5 Å^3. Ni atoms with *ih* and *ih*-like coordinations should then exhibit a remarkably lower mobility than others.

Such inference is supported by an extensive analysis of the dynamics of Ni atoms with *ih* and *ih*-like coordinations in unstrained configurations. It appears that only 5% of the above-mentioned species participates on the average in local rearrangements. This also suggests that rearrangements occur

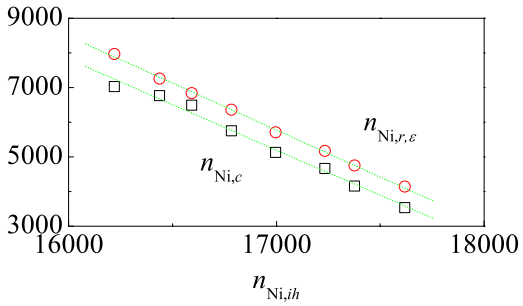

FIG. 11. (Color online) The number of mobile Ni atoms in unstrained configurations, $n_{\mathrm{Ni},c}$, and in configurations strained at a ε_x value of 0.03, $n_{\mathrm{Ni},r,\varepsilon}$, as a function of the number $n_{\mathrm{Ni},ih}$ of Ni atoms with *ih* and *ih*-like coordinations in unstrained configurations. Best-fitted lines are also shown.

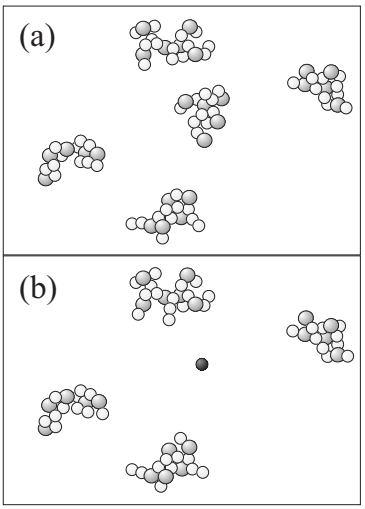

FIG. 12. The Ni (light gray) and Zr (dark gray) atoms involved in cooperative rearrangements in the unstrained configurations that have undergone (a) three and (b) four compression cycles. The isolated atom in the darker gray approximately at the center of (b) is the Ni atom with *ih*-like coordination appeared after the fourth compression cycle.

where Ni atoms do not have *ih* and *ih*-like coordinations. Investigations along such a line were pursued further by monitoring in detail the structural evolution of local atomic arrangements. Useful support in such analysis came from the direct comparison between before mobile atoms and after a given compression cycle. An example is given in Figs. 12(a) and 12(b), which show the Ni and Zr atoms participating in collective motion in unstrained configurations that have undergone three and four compression cycles, respectively. It can be seen that the clusters of mobile atoms involved in displacements as well as their positions after three and four compression cycles are substantially the same, except for the cluster approximately at the center of Fig. 12(a). No collective rearrangement is observed in such position after the fourth compression cycle. Such modification can be apparently ascribed to the appearance of a Ni atom with *ih* or *ih*-like coordinations in the position shown in Fig. 12(b). The same happens for a number of similar cases. A change in the coordination shell of an individual Ni atom seems therefore sufficient to suppress a collective rearrangement. To strengthen this evidence, the distribution $P(r)$ of the distances r between Ni atoms with *ih* or *ih*-like coordinations and the nearest atom participating in a collective rearrangement was calculated. Typical data are shown in Fig. 13, where $P(r)$ is compared with the global PCF of the metallic glass. On the average, Ni atoms with *ih* and *ih*-like coordinations are relatively far from rearranging clusters. Similar data are obtained in all the cases investigated. Accordingly, it can be inferred that such species hinder local cooperative rearrangements.

Based on the findings mentioned above, the effects of compression cycles on the atomic mobility in metallic glasses should be connected with a redistribution of atomic volume. Such a redistribution induces the transformation of structurally unstable regions into more stable ones with an

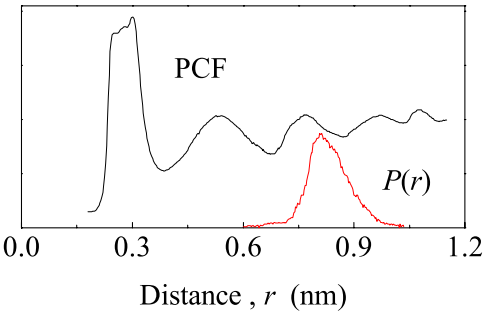

FIG. 13. (Color online) The distribution $P(r)$ of the distances r between Ni atoms with *ih* and *ih*-like coordinations and the nearest atom participating in a collective rearrangement. The data refer to an unstrained configuration that has undergone five compression cycles. The global PCF of the metallic glass is also shown for comparison.

increase in the number of Ni atoms with *ih* and *ih*-like coordinations. The atomic density ρ of the metallic glass should therefore increase with the number m of compression cycles. Since the density ρ increase per compression cycle is quite small, a large number m of compression cycles must be carried out to obtain reliable evidence in this direction. To this specific aim, a smaller $Ni_{50}Zr_{50}$ metallic glass system of about 8000 atoms was generated and subjected to a total of 50 compression cycles. The results obtained are shown in Fig. 14, where the atomic density ρ can be seen to increase as the number m of compression cycles increases. Compression cycles can then be used to stabilize the structure of metallic glasses obtained at high quenching rates.

VII. CONCLUSIONS

An attempt of relating local structural features to cooperative atomic mobility in metallic glasses in the absence and in the presence of elastic shear stress has been carried out. The numerical findings suggest that metallic glasses are complex systems characterized by structural heterogeneity. More specifically, local atomic arrangements exhibit a characteristic degree of stability against structural modifications. This has crucial consequences on the atomic mobility under simple thermal activation in the absence and in the presence of elas-

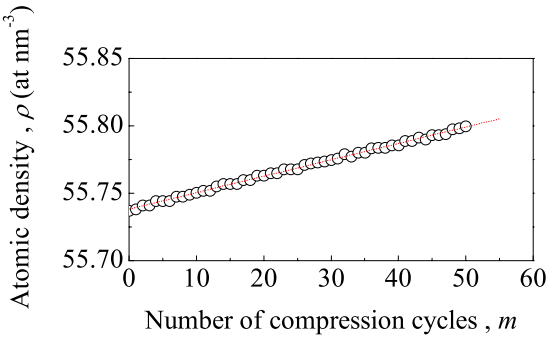

FIG. 14. (Color online) The atomic density ρ of unstrained configurations as a function of the number m of compression cycles. The best-fitted line is also shown.

tic shear stress. The structure of local arrangements can be also modified by hydrostatic compression cycles, which determine a decrease in atomic mobility as a result of a decrease in number and average size of mobile atom clusters. The loss of mobility in unstrained and strained configurations is correlated, with the atoms losing mobility being the same.

The aforementioned behavior can be at least in part ascribed to the increase in the number of Ni atoms with *ih* or *ih*-like coordinations. Characterized by a much lower mobility than others, these latter species represent a serious obstacle to the occurrence of local atomic rearrangements. Since their lower mobility is related to the larger activation volume for diffusion, a significant role of atomic volumes in the occurrence of local atomic rearrangements can be inferred.

The results obtained support the hypothesis that the localization of cooperative displacements in a given region is governed by the relative stability of local atomic arrangements. Being highly improbable to observe a rearrangement in the neighborhood of Ni atoms with *ih* or *ih*-like coordinations, atomic arrangements containing such species cannot be regarded as potential STZs. In contrast, such evidences provide information on what a potential STZ actually should be. In the present case, it can be indeed roughly defined as a small region of metallic glass in which Ni atoms have coordination different from the *ih* or *ih*-like ones and the structural arrangement is unstable against thermal and mechanical perturbations. It is precisely the latter point that needs clarification. A quantity able to quantitatively measure such degree of structural stability should be in fact defined. A response to such question could open the door to an operative classification of local arrangements in unstrained configurations and to a prediction of potential STZs, with an additional information about the temperature and strain conditions at which they could operate.

The emerging scenario of a heterogeneous metallic glass structure with regions specifically hindering local rearrangements entails in principle some relationship to the conceptual framework based on the percolation of short-range order.[38–41] In accordance with previous work,[41] the regions including Ni atoms with *ih* or *ih*-like coordinations undergo exclusively elastic deformation. It seems therefore that the presence of Ni atoms with *ih* or *ih*-like coordinations could represent a necessary condition for a relatively ordered local structuring of atomic species, which could recall the quasicrystalline order observed in the short range in numerical studies.[38–40]

ACKNOWLEDGMENTS

Financial support has been given by the University of Cagliari. A. Ermini, ExtraInformatica s.r.l. is gratefully acknowledged for technical support.

*delogu@dicm.unica.it

[1] W. L. Johnson, MRS Bull. **24**, 42 (1999).
[2] A. Inoue, Acta Mater. **48**, 279 (2000).
[3] W. L. Johnson, JOM **54**, 40 (2002).
[4] A. L. Greer, E. Ma, MRS Bull. **32**, 611 (2007).
[5] C. A. Schuh, T. C. Hufnagel, and U. Ramamurty, Acta Mater. **55**, 4067 (2007).
[6] A. R. Yavari, J. J. Lewandowski, J. Eckert, MRS Bull. **32**, 611 (2007).
[7] D. C. Hofmann, J.-Y. Suh, A. Wiest, G. Duan, M.-L. Lind, M. D. Demetriou, and W. L. Johnson, Nature (London) **451**, 1085 (2008).
[8] F. Spaepen, Acta Metall. **25**, 407 (1977).
[9] A. S. Argon and H. Y. Kuo, Mater. Sci. Eng. **39**, 101 (1979).
[10] A. S. Argon, J. Phys. Chem. Solids **43**, 945 (1982).
[11] P. S. Steif, F. Spaepen, and J. W. Hutchinson, Acta Metall. **30**, 447 (1982).
[12] F. Spaepen and A. Taub, in *Amorphous Metallic Alloys*, edited by F. Luborsky (Butterworths, London, 1983), p. 231.
[13] T.-W. Wu and F. Spaepen, Philos. Mag. B **61**, 739 (1990).
[14] M. L. Falk and J. S. Langer, Phys. Rev. E **57**, 7192 (1998).
[15] M. L. Falk, Phys. Rev. B **60**, 7062 (1999).
[16] A. C. Lund and C. A. Schuh, Acta Mater. **51**, 5399 (2003).
[17] C. A. Schuh and A. C. Lund, Nature Mater. **2**, 449 (2003).
[18] M. L. Falk, J. S. Langer, and L. Pechenik, Phys. Rev. E **70**, 011507 (2004).
[19] J. S. Langer, Scr. Mater. **54**, 375 (2006).
[20] F. Cleri and V. Rosato, Phys. Rev. B **48**, 22 (1993).
[21] C. Massobrio, V. Pontikis, and G. Martin, Phys. Rev. Lett. **62**, 1142 (1989).
[22] F. Delogu and G. Cocco, Phys. Rev. B **74**, 035406 (2006).
[23] I. Ladadwa and H. Teichler, Phys. Rev. E **73**, 031501 (2006).
[24] H. C. Andersen, J. Chem. Phys. **72**, 2384 (1980).
[25] S. Nosé, J. Chem. Phys. **81**, 511 (1984).
[26] M. P. Allen and D. Tildesley, *Computer Simulation of Liquids* (Clarendon Press, Oxford, 1987).
[27] H. Teichler, J. Non-Cryst. Solids **293-295**, 339 (2001).
[28] J. L. Finney, Proc. R. Soc. London, Ser. A **319**, 495 (1970).
[29] H. Mehrer, in *Diffusion in Solid Metals and Alloys*, Landolt Bornstein, New Series, Group III Vol. 26, edited by H. Mehrer, (Springer, Berlin, 1990), p. 1.
[30] H. R. Schober, Phys. Rev. Lett. **88**, 145901 (2002).
[31] F. Faupel, W. Frank, M.-P. Macht, H. Mehrer, V. Naundorf, K. Ratzke, H. R. Schober, S. K. Sharma, and H. Teichler, Rev. Mod. Phys. **75**, 237 (2003).
[32] C. Donati, J. F. Douglas, W. Kob, S. J. Plimpton, P. H. Poole, and S. C. Glotzer, Phys. Rev. Lett. **80**, 2338 (1998).
[33] N. Giovambattista, S. V. Buldyrev, H. E. Stanley, and F. W. Starr, Phys. Rev. E **72**, 011202 (2005).
[34] H. Zhang, D. J. Srolovitz, J. F. Douglas, and J. A. Warren, Phys. Rev. B **74**, 115404 (2006).
[35] Q.-K. Li and M. Li, Appl. Phys. Lett. **88**, 241903 (2006).
[36] K. Brinkmann and H. Teichler, Phys. Rev. B **66**, 184205 (2002).
[37] Ch. Hausleitner and J. Hafner, Phys. Rev. B **45**, 128 (1992).
[38] Y. Shi and M. L. Falk, Phys. Rev. Lett. **95**, 095502 (2005).
[39] Y. Shi and M. L. Falk, Phys. Rev. B **73**, 214201 (2006).
[40] Y. Shi and M. L. Falk, Scr. Mater. **54**, 381 (2006).
[41] M. Wakeda, Y. Shibutani, S. Ogata, and J. Park, Intermetallics **15**, 139 (2007).